

Structure of ^{96}Ru

E. Adamides, J. Sinatkas, L. D. Skouras, and A. C. Xenoulis
Nuclear Research Center Demokritos, Attikis, Greece

E. N. Gazis, C. T. Papadopoulos, and R. Vlastou
Physics Laboratory II, National Technical University of Athens, Athens, Greece
 (Received 5 November 1985)

The level structure and the decay properties of levels in ^{96}Ru up to 3.3 MeV of excitation have been investigated via singles directional-correlation and Doppler-shift measurements following the $^{96}\text{Ru}(p,p'\gamma)$ reaction at 7.0 MeV proton energy. The level and decay scheme of ^{96}Ru was supplemented and clarified on the basis of $\gamma\gamma$ -coincidence measurements. The directional correlations for many transitions provided (i) reliable branching ratios, (ii) J^π assignments, and (iii) multipole mixing ratios $\delta(E2/M1)$ from analysis of the correlations via the compound statistical theory for nuclear reactions. In many cases the measured cross sections helped for a more precise assignment of J^π values. Lifetimes for four states and limits to three additional states were obtained by the Doppler-shift attenuation method from singles spectra, taken in the presence of standards, at eight angles between 0° and 110° to the beam direction. For several transitions in ^{96}Ru values or limits of $B(E1)$, $B(E2)$, and $B(M1)$ were obtained. The levels of ^{96}Ru and their decay properties were calculated in the shell-model framework and are compared with the corresponding experimental quantities.

I. INTRODUCTION

This work reports on a joint experimental and theoretical investigation on ^{96}Ru and is a continuation of a systematic study on the structure of the nuclei in the $A \simeq 90$ region made by member of our group.¹⁻⁷

The level and decay scheme of ^{96}Ru has been studied via the following particle and spectroscopic methods: (α, α') scattering,⁸ decay of $^{96}\text{Rh}^{m,g}$,⁸⁻¹³ $^{92}\text{Mo}(\alpha, 2n\gamma)$ reaction,¹⁴ heavy-ion fusion evaporation reactions^{9,15,16} $(p, p'\gamma)$ (Ref. 17), and Coulomb excitation experiments.^{18,19} From the above studies J^π assignment has been made to several levels in ^{96}Ru . Regarding the electromagnetic properties of transitions in ^{96}Ru , only limited information exists to date. Mixing ratios were measured for seven transitions in this nucleus by Lange *et al.*¹⁷ Lifetimes for the first two excited states and $B(E2)$ rates for the 832.6, 685.5, and 1098.5 keV γ rays deexciting the first three excited states in ^{96}Ru were found by Landsberger *et al.*,¹⁸ while Fahlander *et al.*²⁰ measured the quadrupole moment of the first excited 2^+ state using the reorientation precession technique.

In the present study more light is shed on the structure of ^{96}Ru through detailed $(p, p'\gamma)$ spectrometry. Five new levels at 2579.0, 2700.1, 2987.8, 3210.1, and 3232.1 keV excitation are established, while several γ rays are assigned to the decay of previously known levels on the basis of $\gamma\gamma$ -coincidence measurements. Some inconsistencies that previously appeared between the level and decay scheme rendered from the $(p, p'\gamma)$ reaction of Ref. 17 and the decay studies reported in Refs. 9 and 11 are also clarified in the present work. J^π values and mixing ratios are determined for levels and transitions in ^{96}Ru from singles angular correlations and cross-section measurements following the $(p, p'\gamma)$ reaction with the aid of the Hauser-

Feshbach theory²¹ for compound nucleus reactions. Lifetimes for four states and limits for three others are obtained from Doppler-shift attenuation (DSA) measurements and, finally, $B(\sigma L)$ values for several transitions are determined. A detailed description of the new data established for ^{96}Ru is given in Secs. II, III, and IV of this paper.

There have been several attempts to interpret some properties of the Ru isotopes in terms of nuclear structure models.^{8,14,15,17,18} Ball and Bhatt²² attempted a shell-model calculation on ^{96}Ru using the limited model space of $1p_{1/2}$ and $0g_{9/2}$ orbitals for the protons and the $1d_{5/2}$ orbital for the neutrons. At the time this calculation was reported there were not enough data on ^{96}Ru to allow a detailed comparison between experiment and theory. However, in the light of today's evidence, the calculation of Ball and Bhatt fails to account for the presence of several of the observed levels above 2 MeV of excitation. This feature strongly suggests that for a satisfactory description of the observed ^{96}Ru properties a more extended calculation is required. Such a calculation has recently been reported by Walkiewicz *et al.*⁹ The model space employed by Walkiewicz *et al.*⁹ is similar to that of Ref. 22 for the protons, but for the neutrons they consider configuration mixing in the space of $1d_{5/2}$, $0g_{7/2}$, $2s_{1/2}$, and $1d_{3/2}$ orbitals. The results of this calculation appear to be in very good agreement with experiment with respect to the energy spectrum.⁹ However, Walkiewicz *et al.*⁹ did not calculate the transition rates of ^{96}Ru and thus the comparison between their results and experiment is not complete.

In order to provide some theoretical interpretation of the observed properties of ^{96}Ru we have also attempted an extended shell-model calculation. In this calculation the doubly magic $^{100}_{50}\text{Sn}$ is assumed as inert core and $^{96}_{44}\text{Ru}$ is

described in terms of six proton holes distributed in the $0g_{9/2}$, $1p_{1/2}$, and $1p_{3/2}$ orbitals and two neutrons that are allowed to occupy the $1d_{5/2}$, $0g_{7/2}$, $2s_{1/2}$, and $1d_{3/2}$ orbitals. This model differs from the one employed in our previous calculations in the $A \approx 90$ region²⁻⁵ in the respect that a larger space is employed for the protons. The choice of the proton space made here has been suggested by the results of a calculation⁷ on the $N=50$ and $Z \leq 46$ nuclei. Details on the present calculation together with a comparison between experimental and theoretical results on ^{96}Ru are given in Sec. V of this paper.

II. EXPERIMENTS AND RESULTS

In the present study four types of measurements were performed using the $^{96}\text{Ru}(p,p'\gamma)^{96}\text{Ru}$ reaction. In the first type of experiment, $\gamma\gamma$ coincidences were recorded with two Ge(Li) detectors following the $^{96}\text{Ru}(p,p'\gamma)$ reaction at 7.0 MeV. The second type of experiment involved precise measurements of the energy of the γ rays from the reaction of interest. In the third type of experiment the angular distributions of the γ rays from ^{96}Ru were measured at 7.0 MeV bombardment energy (below the threshold for producing ^{96}Rh) in singles experiments in which levels up to 3.3 MeV were reached. From these experiments branching ratios and cross sections of individual levels in

^{96}Ru were obtained as well as information about spins and multipole mixing ratios. In the last type of measurement the mean lifetimes of levels in ^{96}Ru were obtained via the Doppler shift attenuation method using the $^{96}\text{Ru}(p,p'\gamma)$ reaction at $E_p=7.0$ MeV from singles γ -ray spectra measured between 0° and 110° to the beam in the presence of radioactive sources.

The proton beams were provided by the $T_{11/25}$ Tandem Van de Graaff accelerator of the NRC Demokritos. The target employed was a self-supporting foil 5.0 mg/cm² thick of Ru metal enriched to 97.92% in mass 96. The main contaminants were ^{98}Ru (0.11%), ^{99}Ru (0.43%), ^{100}Ru (0.35%), ^{101}Ru (0.37%), ^{102}Ru (0.55%), and ^{104}Ru (0.27%).

For γ -ray counting two high resolution Ge(Li) detectors with efficiencies 13% and 18.9% and full widths at half maximum (FWHM) of 1.9 keV at 1332 keV were used.

A typical spectrum of the γ rays from the $^{96}\text{Ru}(p,p'\gamma)$ reaction at 7.0 MeV observed at 55° to the beam is shown in Fig. 1.

A. $\gamma\gamma$ -coincidence experiment

In order to clarify and supplement the existing level scheme of ^{96}Ru , we performed a coincidence experiment with the $^{96}\text{Ru}(p,p'\gamma)$ reaction at 7.0 MeV. In this experi-

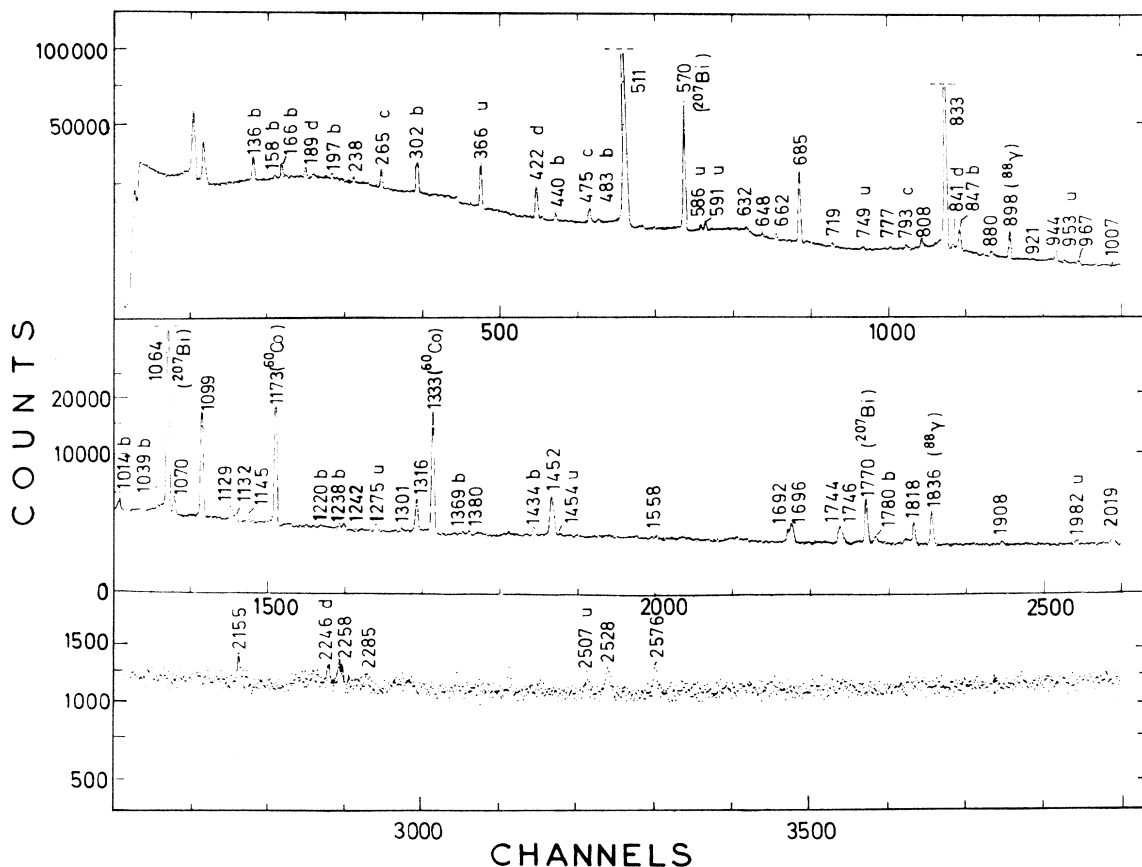


FIG. 1. γ ray spectrum from the reaction $^{96}\text{Ru}(p,p'\gamma)$ at $E_p=7.0$ MeV taken at 55° to the beam direction. In this spectrum the γ rays which belong to the ^{96}Ru scheme are simply indicated by their energy in keV. Peaks due to background radiations, the $^{96}\text{Ru}(p,\gamma)^{97}\text{Ru}$ reaction, the decay of ^{97}Rh , or unidentified radiations are labeled as b, c, d, or u.

TABLE I. Summary of the observed $\gamma\gamma$ -coincidence relationships in the decay of the levels in ^{94}Tc populated in the $^{96}\text{Ru}(p,p'\gamma)$ reaction at $E_p = 7.0$ MeV.

γ -ray energy in the Ge(Li) gate (keV)	γ ray seen in the Ge(Li) coincidence spectrum (keV)
238	685,833,944
487	685,833,1070
648	833,1099
685	238,487,632,833,944,1007,1070,1132, 1182,1242,1380,1478,1558,1692,1744
808	833,1099
833	238,426,487,632,648,685,808,921,944, 967,1070,1099,1129,1132,1145,1242,1301, 1316,1331,1380,1452,1558,1692,1696,1743, 1744,1818,1908,2019,2155,2228,2258,2377, 2429
944	238,685,833
1070	487,685,833
1099	594,648,808,833,921,967,1129,1145,1301 1331
1129	833,1099
1132	685,833
1145	833,1099
1242	685,833
1316	833
1452	777,833
1692	833
1696	833
1818	426,833
1908	833

ment the two Ge(Li) detectors previously mentioned were used at 55° on each side of the beam. Coincidence resolving times of 10 nsec at FWHM were obtained. The total coincidence rate was about 20 counts/sec with the total random rate well below 10%. A total number of 1.8×10^6 coincidence events were measured.

The data were recorded on magnetic tapes in a related address form in a $256 \times 2048 \times 2048$ channel three parameter configuration (Δt , $E1$, $E2$) with the aid of the PDP-11/15 computer. A total of 25 gates were placed on peaks of interest and nearby Compton background in the off line analysis of the data. The established $\gamma\gamma$ -coincidence relationships are summarized in Table I. Some coincidence spectra are shown in Figs. 2 and 3 after background subtraction.

B. γ -ray energy measurements

For the accurate measurement of the γ ray energies following the $^{96}\text{Ru}(p,p'\gamma)$ reaction, the high resolution 18.9% Ge(Li) detector previously mentioned was used. Spectra at 90° to the beam were taken for this purpose at 7.0 MeV bombardment energy in the presence of radioactive sources. Additional measurements of the energy of many γ rays were obtained from the Doppler-shift experiments. The γ -ray energies measured in this work are summarized in column 5 of Table II.

C. Angular distributions and relative level cross sections

Spins of levels, multipole mixing ratios, and branching ratios of electromagnetic transitions were obtained from angular distribution measurements at 7.0 MeV proton energy. In this experiment the 13% and 18.9% Ge(Li) detectors previously mentioned were used. The 18.9% Ge(Li) was used as a movable detector while the 13% was used as a fixed monitor. The anisotropy of the experimental geometry was found to be less than 2% and was neglected. Singles γ -ray spectra were taken at eight detector angles $\theta_d = 0^\circ, 15^\circ, 30^\circ, 45^\circ, 55^\circ, 70^\circ, 90^\circ$, and 110° with respect to the incident proton beam. An effort was made to keep the beam current low and constant during these runs in order to minimize dead time and amplifier pileup corrections. The spectra were normalized with the help of high intensity peaks in the associated spectra of the monitor and with the theoretical angular distribution of the 685.49 keV γ ray deexciting the 4_1^+ state at 1518.1 keV in ^{96}Ru . The obtained angular distributions were first analyzed by a least squares fit of the data to the function.

$$W(\theta_d) = A_0[1 + A_2P_2(\cos\theta_d) + A_4P_4(\cos\theta_d)] \quad (1)$$

The coefficients of the Legendre polynomials obtained in this way were not corrected for solid angle since the latter was so small that it essentially reduced the corresponding geometrical attenuation coefficients to unity. The A_0

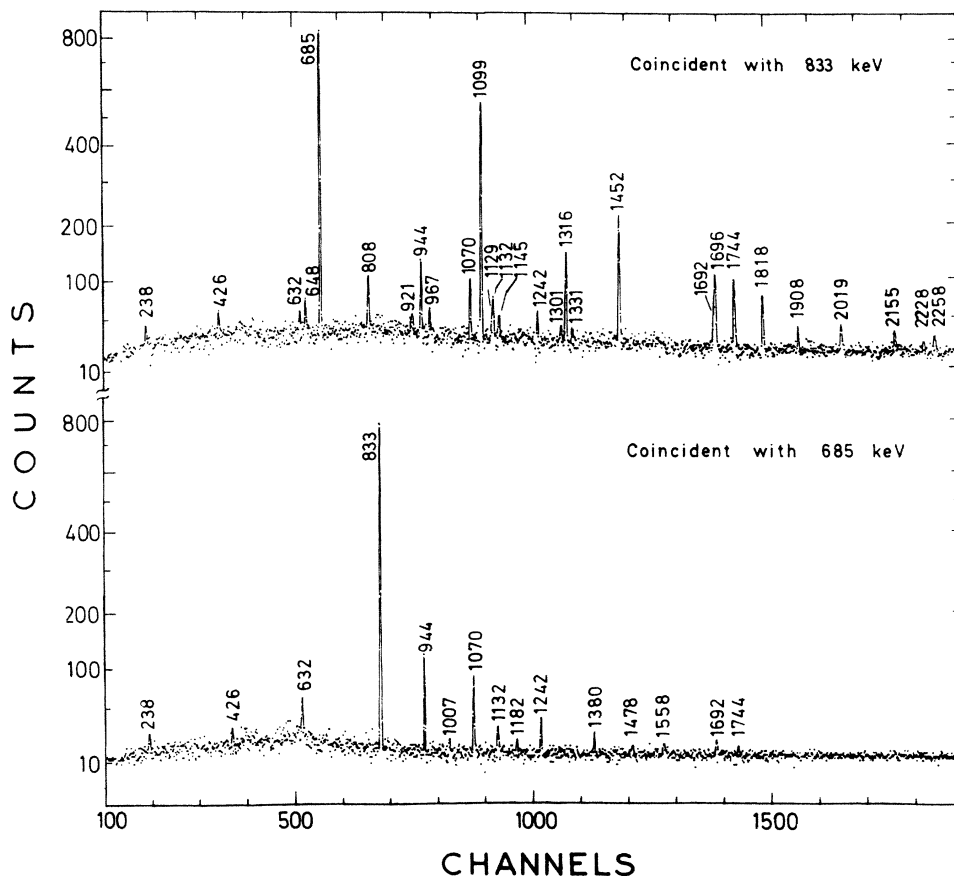


FIG. 2. Spectra of γ rays from the $^{96}\text{Ru}(p,p',\gamma)$ reaction at $E_p=7.0$ MeV in coincidence with the indicated γ -ray peaks. The contribution from the underlying Compton has been subtracted.

values give the branching ratios obtained in column 6 of Table II. The A_2 and A_4 coefficients are given in Table III.

In order to determine the J^π values of levels in ^{96}Ru as well as the multipole mixing ratios δ of the deexciting transitions from the angular distributions, the Hauser-Feshbach theory²¹ for nuclear reactions was employed. The applicability of the statistical theory is ensured in the present experiments since for incident proton energy of 7.0 MeV and a target of 5.0 mg/cm² positioned at 45° to the beam, one obtains an energy spread of 220 keV which is sufficient to average over statistical fluctuations.

The calculation of the theoretical distributions was made with the program MANDYF (Ref. 23) which was modified in order to fit the theoretical distribution to the experimental $W(\theta_d)/A_0$ data and yield an approximate χ^2 as a function of δ . Transmission coefficients for protons were obtained from the penetrability tables of Mani *et al.*²⁴ The distributions were further analyzed with the program MINUIT (Ref. 25) which was modified in this laboratory in a search for a precise χ^2 in which a step in δ of 0.001 was used. The theoretical A_2 and A_4 coefficients are given in Table III below the corresponding experimental quantities. Initial spin values were considered in a range permitted by the modes of decay of the state under consideration only for the transitions the spin of which was not found or was not unambiguously determined by previous studies.^{11,17} The parity values used in the calcu-

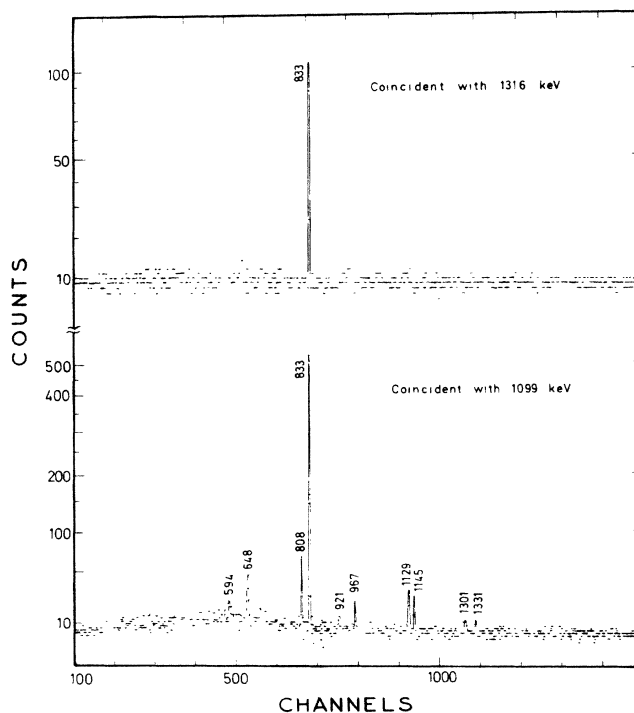


FIG. 3. Spectra of γ rays from the $^{96}\text{Ru}(p,p',\gamma)$ reaction at $E_p=7.0$ MeV in coincidence with the indicated γ -ray peaks. The contribution from the underlying Compton has been subtracted.

TABLE II. Summary of level energies, J^π values, γ -ray energies, and branching fractions for transitions in ^{96}Ru determined in this work.

Level no.	Level energy (keV)	J^π	Transition	γ -ray energy (keV)	Branching (%)
0	0	0^+			
1	832.57 <u>5</u>	2^+	1 \rightarrow 0	832.57 <u>5</u>	100
2	1518.06 <u>7</u>	4^+	2 \rightarrow 1	685.49 <u>5</u>	100
3	1931.08 <u>7</u>	2^+	3 \rightarrow 1	1098.51 <u>5</u>	100
4	2148.80 <u>9</u>	0^+	4 \rightarrow 1	1316.23 <u>7</u>	100
5	2149.77 <u>7</u>	6^+	5 \rightarrow 2	631.71 <u>7</u>	100
6	2284.2 <u>3</u>	2^+	6 \rightarrow 1	1451.6 <u>3</u>	93 <u>3</u>
			6 \rightarrow 0	2284.2 <u>5</u>	7 <u>2</u>
7	2462.4 <u>1</u>	$4,5^+$	7 \rightarrow 2	944.33 <u>9</u>	100
8	2524.6 <u>2</u>	$3^+,4^+$	8 \rightarrow 3	593.8 <u>2</u>	6 <u>2</u>
			8 \rightarrow 2	1006.7 <u>2</u>	9 <u>2</u>
			8 \rightarrow 1	1692.2 <u>2</u>	85 <u>2</u>
9	2528.4 <u>1</u>	$1^+,2^+$	9 \rightarrow 0	2528.4 <u>3</u>	23 <u>3</u>
			9 \rightarrow 1	1695.9 <u>1</u>	77 <u>3</u>
10	2576.1 <u>3</u>	$1^+,2^+$	10 \rightarrow 0	2576.2 <u>3</u>	30 <u>3</u>
			10 \rightarrow 1	1743.4 <u>1</u>	70 <u>3</u>
11	2579.0 <u>3</u>	$0^+,3^+,4^+$	11 \rightarrow 1	(1746.5 <u>2</u>)	63 <u>5</u>
			11 \rightarrow 3	647.9 <u>2</u>	37 <u>4</u>
12	2588.4 <u>1</u>	5	12 \rightarrow 2	1070.36 <u>8</u>	100 <u>2</u>
13	2650.0 <u>2</u>	$2^+,3^-$	13 \rightarrow 1	1817.5 <u>1</u>	74 <u>2</u>
			13 \rightarrow 2	1131.9 <u>2</u>	12 <u>2</u>
			13 \rightarrow 3	718.5 <u>2</u>	14 <u>2</u>
14	2700.1 <u>2</u>	$4^+,5$	14 \rightarrow 2	(1182)	very weak
			14 \rightarrow 7	237.7 <u>2</u>	100
15	2739.8 <u>3</u>	$2^+,3^+$	15 \rightarrow 1	1907.5 <u>3</u>	31 <u>2</u>
			15 \rightarrow 3	808.4 <u>3</u>	69 <u>2</u>
16	2760.5 <u>3</u>	$4^+,5$	16 \rightarrow 2	1242.4 <u>3</u>	100
17	2851.4 <u>2</u>	$2^+,3$	17 \rightarrow 1	2018.8 <u>2</u>	90 <u>5</u>
			17 \rightarrow 3	920.6 <u>5</u>	10 <u>5</u>
18	2897.7 <u>3</u>	$3^+,4^+$	18 \rightarrow 1	2064.7 <u>3</u>	17 <u>7</u>
			18 \rightarrow 2	1379.5 <u>3</u>	31 <u>6</u>
			18 \rightarrow 3	966.8 <u>2</u>	52 <u>6</u>
19	2987.8 <u>3</u>		19 \rightarrow 1	2155.2 <u>3</u>	100
20	2996.1 <u>3</u>		20 \rightarrow 1	2163.5 <u>3</u>	85 <u>2</u>
			20 \rightarrow 2	1478.0 <u>4</u>	15 <u>2</u>
			20 \rightarrow 8	(472)	very weak
21	3060.5 <u>2</u>		21 \rightarrow 1	2228.3 <u>3</u>	14 <u>5</u>
			21 \rightarrow 3	1129.1 <u>2</u>	69 <u>5</u>
			21 \rightarrow 6	776.8 <u>3</u>	17 <u>5</u>
22	3075.9 <u>2</u>	3^-	22 \rightarrow 2	1557.8 <u>3</u>	17 <u>11</u>
			22 \rightarrow 3	1144.8 <u>2</u>	56 <u>16</u>
			22 \rightarrow 12	487.0 <u>5</u>	18 <u>5</u>
			22 \rightarrow 13	425.2 <u>10</u>	9 <u>4</u>
23	3090.2 <u>3</u>		23 \rightarrow 0	3090.2 <u>5</u>	6 <u>2</u>
			23 \rightarrow 1	2257.6 <u>3</u>	94 <u>6</u>
24	3166.8 <u>3</u>		24 \rightarrow 2	1648.7 <u>3</u>	100
25	3210.1 <u>3</u>		25 \rightarrow 1	2377.6 <u>3</u>	39 <u>15</u>
			25 \rightarrow 2	1692.0 <u>3</u>	61 <u>9</u>
26	3232.1 <u>5</u>		26 \rightarrow 3	1301.1 <u>5</u>	100
27	3261.4 <u>4</u>	2^+	27 \rightarrow 0	3262.0 <u>7</u>	13 <u>3</u>
			27 \rightarrow 1	2428.8 <u>4</u>	87 <u>3</u>
			27 \rightarrow 2	(1744)	very weak
			27 \rightarrow 3	(1331)	very weak

TABLE III. Summary of angular distribution analysis for $E_p = 7.0$ MeV.

Transition (keV) $J_i^\pi \rightarrow J_f^\pi$	Experimental theoretical		χ^2	δ
	A_2	A_4		
1931.1 \rightarrow 832.6	-0.167 <u>8</u>	-0.002 <u>10</u>		
1 ⁺ \rightarrow 2 ⁺	-0.091	0.000	31	1.3 \pm 0.3
1 ⁻ \rightarrow 2 ⁺	-0.170	0.000	0.6	3.1 \pm _{-0.7} ^{0.9}
2 ⁺ \rightarrow 2 ⁺	-0.163	-0.012	1.0	-0.72 \pm 0.05
2 ⁺ \rightarrow 2 ⁺	-0.151	-0.035	3.1	-0.5 \pm _{-1.1} ^{0.8}
2 ⁻ \rightarrow 2 ⁺	-0.169	-0.002	0.7	-0.76 \pm 0.06
3 \rightarrow 2 ⁺	-0.170	0.000	0.6	0.04 \pm 0.01
2462.4 \rightarrow 1518.1	0.287 <u>36</u>	0.021 <u>40</u>		
2 \rightarrow 4 ⁺	0.227	0.006	1.5	-0.56 \pm _{-0.31} ^{0.24}
3 \rightarrow 4 ⁺	0.292	0.010	0.6	-0.60 \pm _{-1.20} ^{0.17}
4 ⁺ \rightarrow 4 ⁺	0.297	0.001	0.6	-0.07 \pm _{-0.10} ^{0.12}
4 ⁺ \rightarrow 4 ⁺	0.339	0.068	1.4	0.94 \pm 0.21
4 ⁻ \rightarrow 4 ⁺	0.298	0.002	0.6	-0.10 \pm 0.10
5 \rightarrow 4 ⁺	0.280	0.032	0.6	0.35 \pm 0.05
6 \rightarrow 4 ⁺	0.379	0.103	2.3	0.01 \pm 0.04
2588.4 \rightarrow 1518.1	-0.301 <u>34</u>	0.049 <u>41</u>		
3 ⁺ \rightarrow 4 ⁺	-0.275	0.001	0.8	0.21 \pm 0.07
3 ⁺ \rightarrow 4 ⁺	-0.292	0.034	0.6	9.0 \pm _{-3.5} ^{13.3}
3 ⁻ \rightarrow 4 ⁺	-0.276	0.002	0.6	0.26 \pm 0.09
4 ⁺ \rightarrow 4 ⁺	-0.218	-0.078	2.3	-1.2 \pm _{-0.4} ^{0.2}
4 ⁺ \rightarrow 4 ⁺	-0.205	-0.135	4.1	-42.3
4 ⁻ \rightarrow 4 ⁺	-0.212	-0.088	2.6	-1.1 \pm 0.2
5 \rightarrow 4 ⁺	-0.274	0.000	0.8	-0.01 \pm 0.04
5 ⁺ \rightarrow 4 ⁺	-0.420	0.263	5.7	-3.8 \pm 0.6
5 ⁻ \rightarrow 4 ⁺	-0.395	0.219	3.9	-3.9 \pm 0.6
6 ⁺ \rightarrow 4 ⁺	0.009	-0.365	21	-0.38 \pm 0.06
6 ⁺ \rightarrow 4 ⁺	-0.029	-0.292	15	-2.9 \pm 0.5
6 ⁻ \rightarrow 4 ⁺	0.054	-0.407	26	-0.33 \pm 0.05
2650.0 \rightarrow 832.6	-0.110 <u>26</u>	0.010 <u>31</u>		
1 ⁺ \rightarrow 2 ⁺	-0.092	0.000	0.4	1.3 \pm _{-0.9} ^{6.5}
1 ⁻ \rightarrow 2 ⁺	-0.079	0.000	0.7	0.75 \pm _{-0.6} ^{0.4}
2 \rightarrow 2 ⁺	-0.101	-0.008	0.4	-0.54 \pm 0.11
2 ⁺ \rightarrow 2 ⁺	-0.087	-0.037	0.8	\geq -7.0
3 \rightarrow 2 ⁺	-0.106	0.001	0.4	0.08 \pm 0.04
3 \rightarrow 2 ⁺	-0.186	0.151	4.2	-4.5 \pm 0.8
4 ⁺ \rightarrow 2 ⁺	0.052	-0.205	10.4	-2.2 \pm 0.4
4 ⁻ \rightarrow 2 ⁺	0.079	-0.232	13.4	-2.5 \pm 0.4
2739.8 \rightarrow 1931	0.159 <u>42</u>	0.023 <u>47</u>		
1 \rightarrow 2 ⁺	0.037	0.000	3.2	-0.75 \pm _{-0.9} ^{0.5}
2 \rightarrow 2 ⁺	0.168	0.000	0.5	-0.5 \pm _{-0.12} ^{0.13}
2 \rightarrow 2 ⁺	0.184	0.031	0.7	2.4 \pm _{-0.7} ^{1.1}
3 \rightarrow 2 ⁺	0.161	0.015	0.4	0.32 \pm _{-0.06} ^{0.07}
3 \rightarrow 2 ⁺	0.091	0.160	1.9	$ \delta \leq 50$
4 \rightarrow 2 ⁺	0.268	-0.130	2.5	-0.09 \pm 0.07
4 ⁺ \rightarrow 2 ⁺	0.239	-0.088	1.5	-6.9 \pm _{-5.7} ^{1.2}
4 ⁻ \rightarrow 2 ⁺	0.254	-0.104	1.9	-7.0 \pm _{-4.9} ^{2.1}
2851.4 \rightarrow 832.6	-0.298 <u>42</u>	-0.036 <u>50</u>		
1 ⁺ \rightarrow 2 ⁺	-0.091	0.000	8.0	1.3 \pm _{-0.6} ^{1.4}
1 ⁻ \rightarrow 2 ⁺	-0.199	0.000	2.3	1.3 \pm _{-1.2} ^{1.6}
2 ⁺ \rightarrow 2 ⁺	-0.248	-0.026	0.5	-1.6 \pm _{-1.4} ^{0.6}
2 ⁻ \rightarrow 2 ⁺	-0.246	0.006	0.8	-1.6 \pm _{-1.2} ^{0.6}
3 ⁺ \rightarrow 2 ⁺	-0.332	0.001	0.2	-0.08 \pm _{-0.07} ^{0.06}
3 ⁻ \rightarrow 2 ⁺	-0.317	0.002	0.2	-0.12 \pm _{-0.08} ^{0.07}

TABLE III. (Continued.)

Transition (keV) $J_i^\pi \rightarrow J_f^\pi$	Experimental theoretical		χ^2	δ
	A_2	A_4		
3 \rightarrow 2 $^+$	-0.395	0.136	2.2	$-2.4_{-0.5}^{+0.4}$
4 $^+$ \rightarrow 2 $^+$	-0.051	-0.303	6.9	-1.1 ± 0.4
4 $^-$ \rightarrow 2 $^+$	-0.036	-0.348	8.5	$-1.3_{-0.4}^{+0.6}$
3075.9 \rightarrow 1931.1	-0.317	-0.024		
1 $^+$ \rightarrow 2 $^+$	-0.090	0.000		$\delta \geq 0.2, \delta \leq -4$
1 $^-$ \rightarrow 2 $^+$	-0.199	0.000	0.7	$\delta \geq 0.3, \delta \leq -100$
2 \rightarrow 2 $^+$	-0.249	-0.026	0.3	$-1.6_{-0.9}^{+0.9}$
3 $^+$ \rightarrow 2 $^+$	-0.332	0.001	0.2	$-0.09_{-0.17}^{+0.14}$
3 $^-$ \rightarrow 2 $^+$	-0.332	0.002	0.2	$-0.13_{-0.22}^{+0.16}$
3 \rightarrow 2 $^+$	-0.411	0.136	0.5	$-2.2_{-1.4}^{+0.8}$
4 $^+$ \rightarrow 2 $^+$	-0.052	-0.314	1.6	$-1.1_{-1.0}^{+0.6}$
4 $^-$ \rightarrow 2 $^+$	-0.035	-0.360	2.0	-1.4 ± 1.0

lations are indicated also in Table III. The parity is not given when no significant difference in the results was obtained by parity change. The minimum χ^2 value divided by the degrees of freedom, and the corresponding δ value at the minimum, are contained in the fourth and fifth columns of Table III. The uncertainties quoted with the δ values refer to the 95.5% confidence limit and are evaluated according to the procedure prescribed by Rogers.²⁶ The mixing ratio δ is defined in terms of emission matrix elements according to Krane and Steffen.²⁷

In some cases the comparison of the experimental cross section for direct formation of a level with the predictions of the statistical theory helped in uniquely determining the J^π values. The experimental cross sections were obtained by summing the intensities of the γ rays deexciting a level and subtracting the feeding from higher lying states. The uncertainty in the absolute efficiency of the detector produced large errors in the determination of the absolute level cross sections. For this reason the relative cross sections were normalized to the theoretical value of the cross section as obtained by the statistical model calculations of the 1931 keV level, the spin of which was uniquely established as 2 $^+$ by the present and previous¹⁷ angular correlation measurements. In Fig. 4 histograms of the theoretical cross sections versus spin and parity assumptions of individual levels are compared with the experimental data from the $E_p=7.0$ MeV measurement. The limit for spin rejection was set at 3.3 times the error in the measured cross section.

D. Lifetime measurements

Mean lifetimes of levels in ^{96}Ru were measured via the DSA method from singles γ ray spectra obtained between 0 $^\circ$ and 110 $^\circ$ to the beam at 7.0 MeV using the centroid shift technique. Briefly, the centroid shift is given by

$$\langle \Delta E_\gamma \rangle = E_\gamma^0 \beta_{c.m.} \tilde{F}(\tau) \cos\theta_d, \quad (2)$$

$$\tilde{F}(\tau) = F(\tau) \beta(0) \cos\theta_N W(\theta_N, \theta_d) d\Omega(\theta_N) / \beta_{c.m.}, \quad (3)$$

and

$$F(\tau) = [\beta(0)\tau]^{-1} \int_0^\beta \beta(t) \cos\phi(t) \exp(-t/\tau) dt, \quad (4)$$

where $F(\tau)$ is the attenuation factor averaged over all initial velocities of the recoil nucleus by employing the angular correlation function $W(\theta_N, \theta_d)$ as a weighting factor according to Moazed *et al.*,²⁸ and $\cos\phi(t)$ is the average collision cosine as given by Blaugrund.²⁹ For the calculation of $\beta(t)$ the stopping power theory of Lindhard, Scharff, and Schiott,³⁰ as modified by Blaugrund,²⁹ was used with the stopping power taken as

$$T_t = f_e T_e + f_n T_n, \quad (5)$$

where T_t is the total stopping power, e and n refer to electronic and nuclear stopping powers, and f_e and f_n are adjustable parameters. The lifetimes reported in this work were obtained with $f_e = f_n = 1.0$.

Singles spectra were obtained at eight angles of observation $\theta_d = 0^\circ, 15^\circ, 30^\circ, 45^\circ, 55^\circ, 70^\circ, 90^\circ, 110^\circ$ with respect to the beam direction. Due to the low initial recoil velocity, the observed shifts are very small. In order to obtain accurate results for the centroid positions of the γ rays the spectra were accumulated with internal standards. Care was also taken to keep the beam current low and steady to avoid rapid changes in the energy stability of the system.

The centroid shifts measured in this work for transitions in ^{96}Ru are plotted vs $\cos\theta_d$ in Fig. 5, where the γ -ray energies are given in keV. The straight lines in Fig. 5 were obtained as weighted, least-square fits to the data. The slopes obtained are given in parentheses in keV and correspond to the shifts of Eq. (2) for $\cos\theta_d = 1$. From the slopes the experimental values for $\tilde{F}(\tau)$ were calculated using Eq. (2) and are summarized in the fourth column of Table IV. In the first two columns of Table IV the level numbers and level energies are given. The third column gives the γ rays used in the DSA measurements. The fifth column gives the presently determined mean lifetime in psec for the corresponding levels in ^{95}Ru . These were

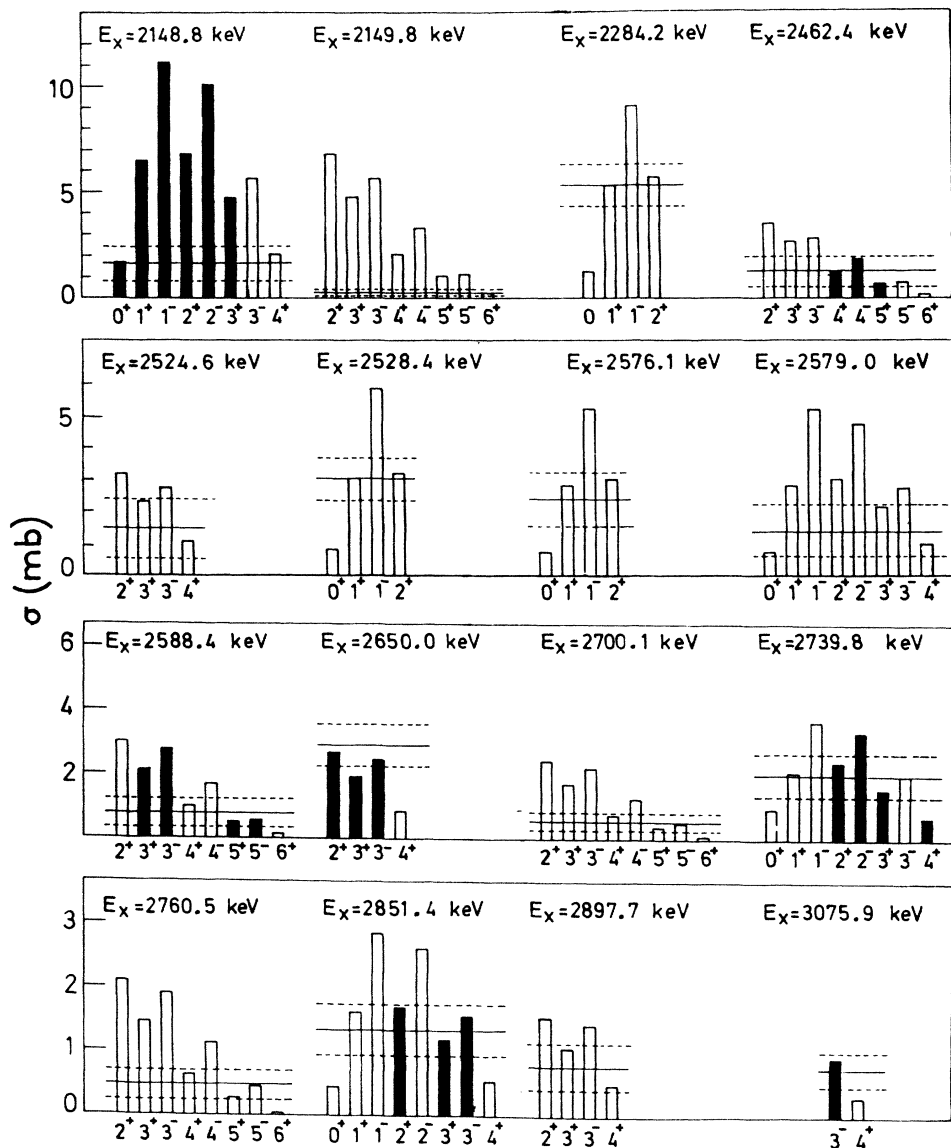


FIG. 4. Histograms of theoretical cross sections versus the spin and parity of levels in ^{96}Ru . Black boxes indicate spin assignment made on the basis of measured angular distribution data combined with other available data. The horizontal central lines are the experimental level cross section. Broken lines indicate the 0.1% (3.3 times the error) rejection limit. The data are taken from the angular distribution experiment at $E_p = 7.0$ MeV.

deduced from a comparison with the theoretical $\tilde{F}(\tau)$ curves as a function of τ , evaluated for each level from Eq. (3). The uncertainties quoted with the present τ values include the statistical error and the effect of a 20% uncertainty in the stopping power. The last column of Table IV gives the previously determined mean lifetimes for the first two excited states in ^{95}Ru (Ref. 18).

III. REDUCED TRANSITION PROBABILITIES IN ^{96}Ru

From the measured branching ratios, multipole mixing ratios, and the level lifetimes presented in Tables II–IV, the reduced transition probabilities for several transitions in ^{96}Ru were deduced. These values are summarized in the last two columns of Table V. The $B(E2)$, $B(M1)$, and

$B(E1)$ values are given in Weisskopf units (W.u.) and are calculated via the expression given in the Appendix of Ref. 31.

IV. STRUCTURE OF ^{96}Ru AND DISCUSSION

The level and decay scheme of ^{96}Ru deduced from our $\gamma\gamma$ -coincidence measurements is presented in Fig. 6. In its main features, this scheme is consistent with the previously existing one.^{9,11,17} However some differences do exist which together with new results and clarification on the structure of ^{96}Ru are discussed in the respective paragraph below.

The state at 1931.08 keV was assigned by Lange *et al.*¹⁷ to have as most probable spin the value 2^+ on the basis of their $\gamma\gamma$ -angular correlation measurements for the 1099-

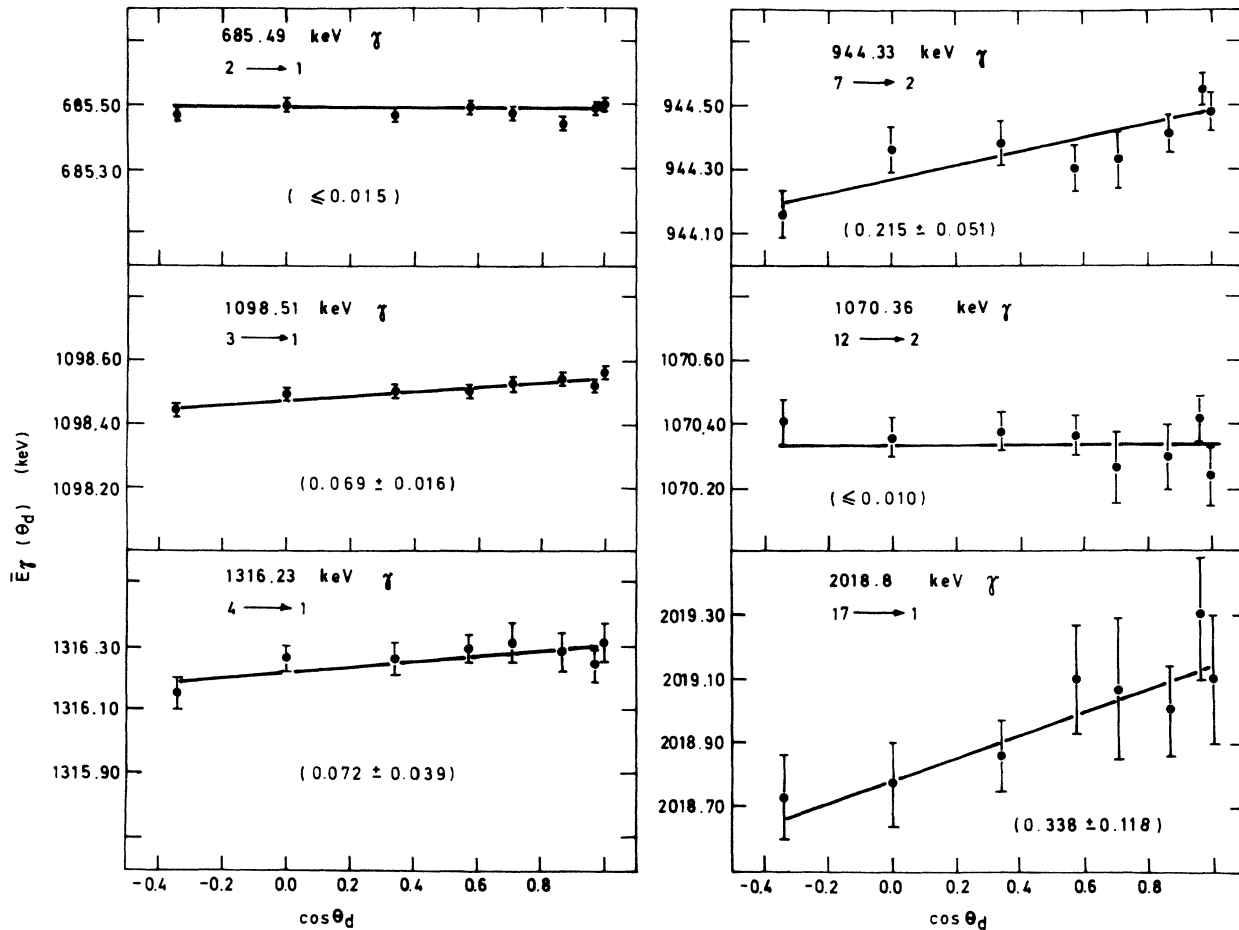


FIG. 5. Plots of centroid energy in keV for the indicated γ rays from ^{96}Ru observed in singles measurements vs $\cos\theta_d$. The integers identify each transition with the entries of Table II. The numbers in parentheses are the least-squares slopes for a straight line fit to the data. Data at $E_p=7.0$ MeV.

833 cascade, although the 1^+ spin value was still possible. Their argument for the exclusion of the 1^+ alternative was based on the systematic trend of neighboring nuclei and on their $p\gamma$ angular correlations starting from the level at 2578 keV. In the present study the 2578 keV level proposed by Lange *et al.*¹⁷ is not adopted. Instead two close lying levels at 2576.1 and 2579.0 keV are assigned as

will be discussed below. The mixing ratio for the 1098.5 keV γ ray deexciting in 1931.08 keV state to the 2_1^+ at 832.57 keV was found in Ref. 17 to be $4.2^{+2.2}_{-1.4}$, although from Fig. 4 of Ref. 17 it is observed that a value of -0.9 cannot be excluded. It is interesting to mention that the mixing ratio of the 992.8 keV $2_2^+ \rightarrow 2_1^+$ transition of the nearby even-even ^{94}Mo nucleus was found² to be

TABLE IV. Summary of the lifetimes for levels in ^{96}Ru measured by the Doppler-shift-attenuation method together with previously available data.

Level no.	E_{level} (keV)	γ ray used in DSA experiment	$\tilde{F}(\tau)$	τ (psec)	
				Present ^a	Previous ^b
1	833				3.9 ± 0.3
2	1518				10.0 ± 1.3
3	1931	1099	0.050 <u>12</u>	$0.55^{+0.22}_{-0.16}$	
4	2149	1316	0.043 <u>24</u>	$0.66^{+0.91}_{-0.26}$	
9	2462	944	0.181 <u>43</u>	$0.14^{+0.07}_{-0.04}$	
12	2588	1070	≤ 0.007	≥ 4.0	
17	2851	2019	0.133 <u>47</u>	$0.20^{+0.14}_{-0.07}$	

^aThe quoted errors include statistical errors and the effects of a 20% uncertainty in the stopping power.

^bReference 18.

$-0.87_{-0.17}^{+0.09}$. Since the 1931.08 keV second excited state is crucial in the clarification of the structure of ^{96}Ru , the spin of this state and the mixing ratio of the deexciting transition have been unambiguously reestablished in this work. From Table III it is seen that the angular distribution of the 1098.5 keV γ ray rules out the $1^+ \rightarrow 2^+$ possibility leaving only the 2^+ value for the spin of the 1931.08 keV state. From the same table it is seen that two δ values are possible for the 1098.5 keV γ ray: $\delta = -0.72 \pm 0.05$ and $\delta = -5.5_{-1.1}^{+0.8}$. From these two values and the lifetime of the 1931.08 keV state measured here to be $0.55_{-0.16}^{+0.22}$ psec the $B(E2)$ rates were calculated as 12_{-4}^{+3} and 33_{-10}^{+14} W.u., respectively. Only the second value is consistent with the $B(E2)$ rate of 34.8 ± 5.0 W.u. found for the 1098.5 keV γ ray from Coulomb excitation experiments.¹⁸ This enables the unique determination of the mixing ratio of the 1098.5 keV transition at $\delta = -5.21_{-1.35}^{+0.98}$ (average value of the presently and previously determined relevant values). So in going from ^{94}Mo to ^{96}Ru the $E2$ component of the $2_2^+ \rightarrow 2_1^+$ transition increases from 51% to 96%, but because this transition is faster⁵ in ^{94}Mo it comes out to have almost the same rate in both nuclei.

The 2148.80 keV state was assigned by Lange *et al.*¹⁷ to have a tentative spin value of 0^+ . In the present work the angular distribution of the 1316.23 keV γ ray deexciting this state to the 832.57 keV level was found to be isotropic, as in Ref. 17, and in combination with the direct cross section to the 2148.80 keV state (Fig. 4) uniquely determines a 0^+ spin value for this level. From Table IV it is seen that the $B(E2; 0_2^+ \rightarrow 2_1^+)$ value measured here does not satisfy the phonon-model prediction^{32,33} which is

$$B(E2; J \rightarrow 2^+) / B(E2; 2^+ \rightarrow 0^+) = 2.0$$

for $J = 0^+, 2^+, 4^+$. The same conclusion applies for the $4_1^+ \rightarrow 2_1^+$ transition while for the $2_2^+ \rightarrow 2_1^+$ transition there is a fair agreement with the phonon model. Clear deviations from the classically vibrational expectation are also observed in the heavier Ru isotopes.¹⁸

The 2149.77 keV level deexcites by the 631.71 keV γ ray to the 1518.06 keV level. Lederer *et al.*¹⁴ and Piel and Scharff Goldhaber¹⁵ assigned a spin of 6^+ to this level on the assumption of stretched downward cascades. In this work the spin of 6^+ is uniquely determined on the basis of the measured cross section to the 2149.77 keV level (Fig. 4).

The 2284.2 keV level was found in this work to decay by the 1451.6 and 2284.2 keV γ rays to the 832.57 keV level and the ground state, respectively, in agreement with Ref. 9. The coincidence of the 1451.6 keV γ ray with the 832.57 keV gate is clearly observed in this work (Fig. 2) while in Table 2 of Ref. 11 containing the γ rays in coincidence with the 832.57 keV γ ray the 1451.6 keV γ ray is placed in parentheses. The assignment of the 2284.2 keV γ ray was based on good energy agreement. In Ref. 17 the energy of the 1451.2 keV γ ray was miscalculated. The spin of the 2284.2 keV level was uniquely determined by Lange *et al.*¹⁷ as 2^+ from the analysis of their $p\gamma$ angular correlation data. This spin assignment is consistent with our cross section data (Fig. 4).

The 2462.4 keV level deexcites by the 944.33 keV γ ray

TABLE V. Summary of the electromagnetic properties of transitions in ^{96}Ru .

Transition	Transition energy (keV)	$J_i \rightarrow J_f$	Multipole mixing ratio ($E2/M1$)			$B(E2)$ or $B(M2)$ (in W.u.)	$B(M1)$ or $B(E1)$ (in W.u.)
			Present	Previous ^a	Proposed		
1 \rightarrow 0	832.6	$2^+ \rightarrow 0^+$	$E2$	$E2$	$E2$	20.4 ± 2.0^b	
2 \rightarrow 1	685.5	$4^+ \rightarrow 2^+$		0.016 28	$E2$	20.9 ± 2.8^b	
3 \rightarrow 1	1098.5	$2^+ \rightarrow 2^+$	$-5.5_{-1.1}^{+0.8}$	$-4.2_{-2.2}^{+1.4}$	$-5.2_{-1.4}^{+1.0}$	34_{-10}^{+14}	0.002 1
4 \rightarrow 1	1316.2	$0^+ \rightarrow 2^+$	$E2$	$E2$	$E2$	12_{-7}^{+8}	
7 \rightarrow 2	944.3	$4^+ \rightarrow 4^+$	$-0.07_{-0.10}^{+0.12}$ or 0.94 ± 0.21		$-0.07_{-0.10}^{+0.12}$ or 0.94 ± 0.21	$1.5_{-1.5}^{+7.0}$ 140_{-59}^{+61}	$0.27_{-0.09}^{+0.11}$ $0.14_{-0.04}^{+0.06}$
12 \rightarrow 2	1070.4	$4^- \rightarrow 4^+$ $5^+ \rightarrow 4^+$ $5^- \rightarrow 4^+$	-0.10 ± 0.10 0.35 ± 0.05 -0.01 ± 0.04		-0.10 ± 0.10 0.35 ± 0.05 -0.01 ± 0.04	≤ 200 32_{-14}^{+15} ≤ 1.1	$0.0039_{-0.0013}^{+0.0016}$ $0.24_{-0.08}^{+0.10}$ ≤ 0.09
17 \rightarrow 1	2018.8	$5^+ \rightarrow 4^+$ $2^+ \rightarrow 2^+$ $3^+ \rightarrow 2^+$	-0.01 ± 0.04 -0.01 ± 0.04 $-1.6_{-0.4}^{+0.6}$ $-0.08_{-0.07}^{+0.06}$		-0.01 ± 0.04 -0.01 ± 0.04 $-1.6_{-0.4}^{+0.6}$ $-0.08_{-0.07}^{+0.06}$	≤ 0.01 3.0 ± 1.6 $0.03_{-0.03}^{+0.00}$ $3.6_{-1.5}^{+2.0}$	≤ 0.01 $0.005_{-0.003}^{+0.005}$ $0.017_{-0.008}^{+0.010}$ 0.0026 ± 0.0014
		$3^- \rightarrow 2^+$	or $-2.4_{-0.5}^{+0.4}$ $-0.12_{-0.08}^{+0.07}$		$-2.4_{-0.5}^{+0.4}$ $-0.12_{-0.08}^{+0.07}$	$4.0_{-3.7}^{+8.5}$	$(2.4_{-1.0}^{+1.4}) \times 10^{-4}$

^aReference 17.

^bReference 18.

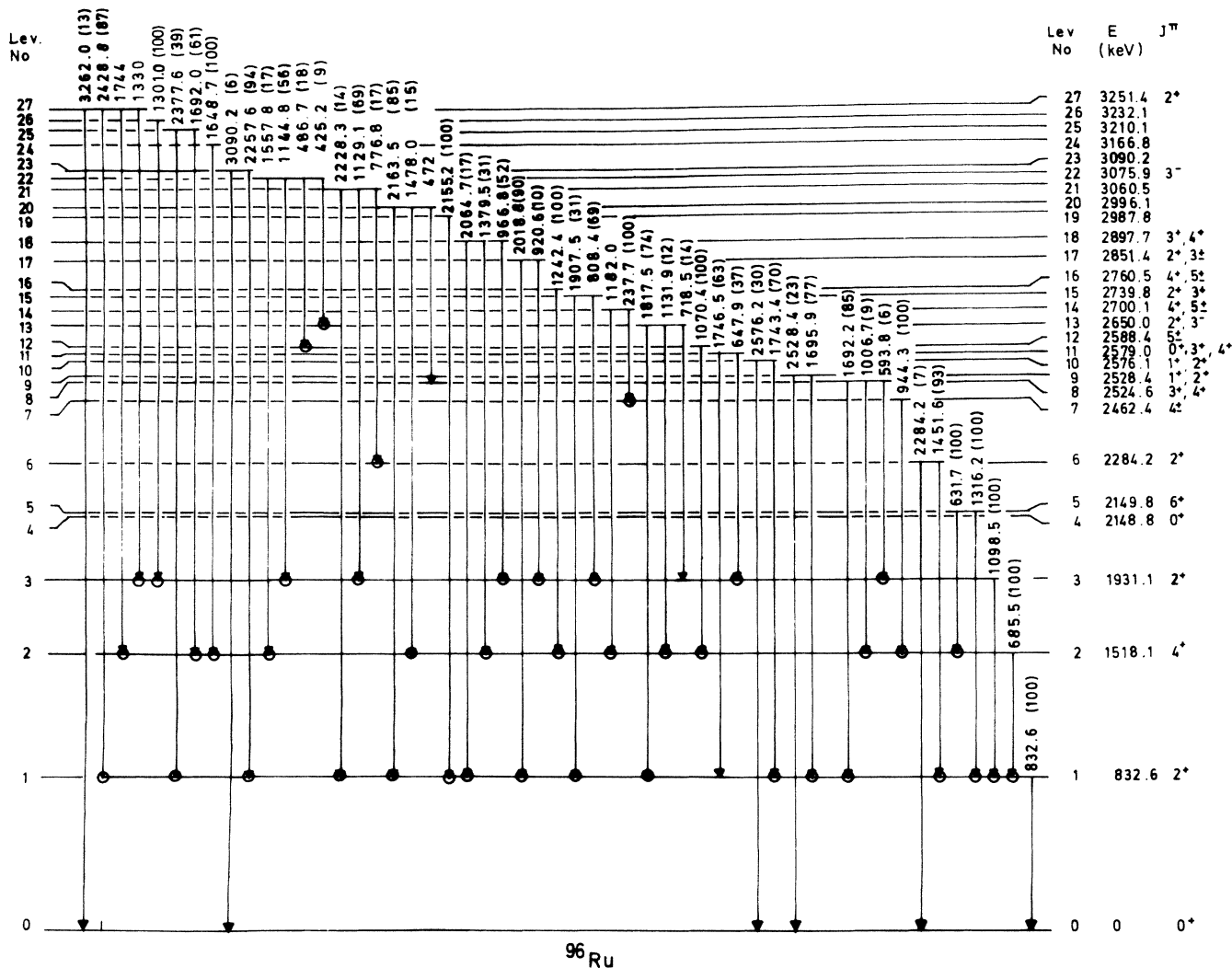


FIG. 6. Proposed scheme for the decay of levels in ^{96}Ru following excitations via the $^{96}\text{Ru}(p,p',\gamma)$ reaction. The energies are in keV and the numbers in parentheses are the present branching fractions for γ decay. The open circles indicate coincidence relationships.

to the 1518.06 keV level. The spin of this state was tentatively assigned as 3 or 4 in Ref. 17 and as 4^{+} in Ref. 9. In the present study the angular distribution of the 944.33 keV γ ray was found consistent with all the possible spin values for the 2462.4 keV level permitted by its modes of decay (Table III). From the lifetime of this level which was found here to be $0.14^{+0.07}_{-0.04}$ psec, and the mixing ratio determined from the analysis of the 944.33 keV correlation the 3^{-} and 5^{-} possibilities can be excluded because they would result in an unlikely high $B(M2)$ value. The 2^{+} and 6^{+} values can also be rejected as they would result in an improbably high $M3$ and $E2$ transition strength for the 944.33 keV γ ray, respectively. From the remaining 3^{+} , 4^{\pm} , or 5^{+} possibilities for the 2462.4 keV level the comparison of the measured direct cross section to this level with the statistical model prediction (Fig. 4) helps to select only the 4^{\pm} or 5^{+} .

The 2462.4 keV level deexcites by the 944.33 keV γ ray to the 1518.06 keV level. The spin of this state was tentatively assigned as 3 or 4 in Ref. 17 and as 4^{+} in Ref. 9. In the present study the angular distribution of the 944.33

1098.51 keV γ ray is clearly observed in this work (Fig. 3) in contradiction with Ref. 11 where the 593.8 keV γ ray was not placed to deexcite the 2524.6 keV level. The 2524.6 keV level was missed by Lange *et al.*¹⁷ The measured direct cross section to this level (Fig. 4) is consistent with a spin value of 3^{+} or 4^{+} .

The level of 2528.4 keV is assigned here to deexcite by the 2528.4 and 1695.9 keV γ rays to the ground state and to the 832.57 keV level, respectively, in agreement with Ref. 17. This level is not populated in the decay of $^{96}\text{Rh}^{m,g}$ studied in Refs. 9 and 11. Improved branching ratios were found in the present study in comparison with Ref. 17. The measured cross section for the 2528.4 keV level determines a spin value of 1^{+} or 2^{+} for this level (Fig. 4).

The level of 2576.1 keV is found in the present work to decay by the 2576.2 and 1743.4 keV γ rays to the ground state and the 832.57 keV level in agreement with Refs. 9 and 11. The comparison of the measured direct cross section to the 2576.1 keV level with the prediction of the statistical model (Fig. 4) determines the spin of this level as

1^+ or 2^+ .

The 2579.0 keV level is assigned in this work on the basis of a 647.9 keV γ ray observed in coincidence with the 1098.51 and 832.57 keV γ rays and placed to deexcite this level to the 1931.08 keV level. A second γ ray at 1746.5 keV is assigned to decay from the 2579.0 keV level to the 832.57 keV level mainly on the basis of good energy agreement. The 1746.5 keV γ ray is a close doublet with the 1743.4 keV γ ray described in the previous paragraph and was not clearly discriminated in the spectrum in coincidence with the 832.57 keV gate. The 2579.0 keV level is not populated in the decay of $^{96}\text{Rh}^{m.g}$ studied in Refs. 9 and 11. We do not agree with Lange *et al.*¹⁷ who assigned a level at 2577.6 keV instead of the close lying levels at 2576.1 and 2579.0 keV described above. The modes of decay of the 2579.0 keV state limit its spin to 0^+ , 1^\pm , 2^\pm , 3^\pm , or 4^+ . The measured cross section to this level (Fig. 4) is consistent with 0^+ , 3^+ , or 4^+ J^π values.

The state of 2588.4 keV deexcites by the 1070.36 keV γ ray to the 1518.06 keV level. The spin of this level was assigned by Lederer *et al.*¹⁴ as 5^- from the angular distribution of the 1070.36 keV γ ray on the assumption of stretched downward cascades and the energy systematics of the 5^- states in even Mo and Ru isotopes. In the present study the angular distribution of the 1070.36 keV γ ray is found consistent with 3^\pm , 4^\pm , or 5^\pm J^π values for the 2588.4 keV level. The 4^- spin can be excluded because it would result in an improbably high $M2$ transition strength for the 1070.36 keV γ ray. The 4^+ value can also be rejected on the 20% confidence limit. The cross section data reject the 3^\pm possibilities leaving only the 5^\pm values as probable spin for the 2588.4 keV level.

The 2650.0 keV level is found to decay by the 1817.5, 1131.9, and 718.5 keV γ rays to the 832.57, 1518.06, and 1931.08 keV levels, respectively, in agreement with Lange *et al.*¹⁷ Improved level and γ -ray energies are found in the present study in comparison with the results of Ref. 17. This level was not assigned in the decay studies.^{9,11} The modes of decay of the 2650.0 keV level limit its spin to 2^+ , 3^\pm , or 4^+ . The angular distribution of the 1817.5 keV γ ray (Table III) rejects the 4^+ possibility. From the remaining 2^+ or 3^\pm J^π values the production cross section to the 2650.0 keV level selects only the 2^+ or 3^- .

A new level at 2700.1 keV has been established by a γ ray at 237.7 keV which was assigned to deexcite this level to the 2462.4 keV level below. This γ ray was seen in coincidence with the 944-685-833 keV cascade. A second weak γ ray at 1182.0 keV was assigned to deexcite the 2700.1 keV level to the 1518.06 keV level on the basis of the observed coincidence of this γ ray with the 685.49 keV gate. The cross section data are consistent with a J^π assignment of 4^+ or 5^\pm for the 2700.1 keV level.

The 2739.8 keV level deexcites by the 1907.5 and 808.4 keV γ rays, respectively. Gujarthi *et al.*¹¹ have proposed tentatively the spin 1^+ , 2^+ , or 3^+ for the 2739.8 keV level since it was populated in the decay of the low spin isomer of ^{96}Rh . The modes of decay of this level limit its spin to 0^+ , 1^\pm , 2^\pm , 3^\pm , or 4^+ . In the present work the angular distribution of the 804.4 keV γ ray (Table III) is consistent with 2^\pm , 3^\mp , or 4^+ J^π values. The 3^- possibility is excluded because it would result in an unlikely high $M2$

contribution. From the remaining 2^\pm , 3^+ , and 4^+ values the measured direct cross section to the 2739.8 keV level helps to select the 2^+ or 3^+ spin values for this level.

The 2760.5 keV level decays by the 1242.4 keV γ ray to the 1518.06 keV level. Our cross section data are consistent with a 4^+ or 5^\pm spin assignment for this level.

The 2851.4 keV level decays by the 2018.8 and 920.6 keV γ rays to the 832.57 and 1931.08 keV levels, respectively. A better assignment of the level and γ -ray energies was made in the present (p,p' γ) work in comparison with Ref. 17. This level was not populated in the study^{9,11} of the decay of $^{96}\text{Rh}^{m.g}$. The lifetime of the 2851.4 keV level was determined here to be $0.20_{-0.07}^{+0.14}$ psec. The angular distribution of the 2018.8 keV γ ray (Table III) is consistent with a 1^- , 2^\pm , or 3^\pm J^π assignment for this level. From the lifetime of the 2851.4 keV level and the mixing ratio determined from the analysis of the 2018.8 keV correlation, the 1^- and 2^- possibilities can be excluded because they would result in an unlikely high $B(M2)$ value for the 2018.8 keV γ ray. The remaining 2^+ or 3^\pm spin values for the 2851.4 keV level are consistent with the cross section data (Fig. 4).

The level at 2897.7 keV was found in the present study to deexcite by the 2064.7, 1379.5, and 966.8 keV γ rays to the 832.57, 1518.06, and 1931.08 keV levels, respectively. The 1379.5 keV γ ray was not assigned in the previous studies^{9,17} and its placement here was based on the coincidence of this γ ray with the 658-833 cascade. In Ref. 17 only the 2064.7 and 966.8 keV γ rays were assigned while in Ref. 9 only the 966.8 keV γ ray was observed to decay from the 2897.7 keV level. This level was totally missed in Ref. 11. The modes of decay of the 2897.7 keV level limit its spin to 2^+ , 3^\pm , or 4^+ . Our cross section data are consistent with a 3^+ or 4^+ J^π assignment.

A new level at 2987.8 keV was established in the present work on the basis of a γ ray at 2155.2 keV which was assigned to decay from this to the 832.57 keV level. This γ was seen in coincidence with the 832.57 keV gate. The level at 2996.2 keV was well established in Refs. 9 and 11.

The 3060.5 keV level was assigned in the (p,p' γ) work of Lange *et al.*¹⁷ A new γ ray at 2228.3 keV is placed to decay from this level to the 832.6 keV level on the basis of its coincidence with the 832.6 keV gate. Improved level energy, γ -ray energies and branching ratios are found in present work in comparison with Ref. 17.

The next level at 3075.9 keV was also established in Ref. 17. In the present study two new γ rays at 1557.8 and 425.2 keV were assigned to deexcite this level to the 1518.06 and 2650.0 keV levels. The 1557.8 keV γ ray was observed in coincidence with the 686-833 cascade while the 425 keV γ ray with the 1818-833 cascade. The modes of decay of this level limit its spin to 3^- or 4^+ . The angular distribution of the 1144.8 keV γ ray is consistent with both spins, although with the 3^- J^π value for the 3075.9 keV level the shape of this distribution is much closer to the experimental results. The 4^+ alternative can also be excluded because it would result in an improbably high $M3$ transition strength for the 1144.8 keV γ ray. Thus only the 3^- assignment remains for the 3075.9 keV level. This spin is consistent with the measured produc-

tion cross section for this level (Fig. 4).

The next two lines at 3090.4 and 3166.8 keV were well established in Refs. 9 and 11.

A new level at 3210.1 keV is assigned here on the basis of two γ rays at 2378 and 1692 keV which were placed to decay from this level to the 832.57 and 1518.06 keV levels below. These two γ rays were found in coincidence with the 832.57 and 685.49 keV gates, respectively.

The last level at 3261.4 keV was well assigned in Refs. 9 and 11. The modes of decay of this state help to uniquely determine its spin as 2^+ .

As can be seen from Fig. 6, most of the levels in ^{96}Ru proceed mainly to the first, second, and third excited states. This is an evidence against vibrationally in which case transitions are mainly made between levels differing by one phonon energy. Single particle excitations in ^{96}Ru can also be evidenced from the $B(E2)$ transition rates (Table IV) for the 2588.4 and 2851.4 keV states which are only slightly greater than the single particle estimates.

V. COMPARISON WITH THEORY

In this section we describe a shell-model calculation on ^{96}Ru and compare its results with the experimental data discussed in Secs. II to IV of this work.

In our calculation the double closed nucleus $^{100}_{50}\text{Sn}$ is assumed as an inert core and $^{96}_{44}\text{Ru}$ is described in terms of six proton holes and two neutron particles attached to this core. The proton holes are placed in the $0g_{9/2}$, $1p_{1/2}$, and $1p_{3/2}$ orbitals. This choice of model space for the protons has been found⁷ to account satisfactorily for the properties of the nuclei with $N=50$ and $42 \leq Z \leq 46$. On the other hand for the neutrons we have adopted the choice of model space made in earlier shell-model calculations in this mass region²⁻⁵ and placed them in the $1d_{5/2}$, $0g_{7/2}$, $2s_{1/2}$, and $1d_{3/2}$ orbitals. Harmonic oscillator wave functions are used throughout the calculation and the harmonic oscillator parameter $b = (\hbar/m\omega)^{1/2}$ is given an appropriate for this mass region value of 2.1 fm.

The number of valence particles and holes together with the number of orbitals included in the model space combine to produce very large dimensions for the energy matrices. For this reason the weak-coupling approximation has been adopted. Thus the total Hamiltonian is conveniently expressed as

$$H = H_p + H_n + V_{pn}, \quad (6)$$

where H_p and H_n describe the effective Hamiltonian in the proton and neutron space, respectively, while V_{pn} denotes the effective interaction between proton holes and neutrons. Assuming full configuration mixing in both proton and neutron spaces, H_p and H_n have been separately diagonalized and their resulting eigenvectors have been combined to form the basis for the ^{96}Ru calculation. Thus the ^{96}Ru basis vectors are expressed as

$$|^{96}\text{Ru}; JM\rangle = |\mu_p J_p, \mu_n J_n; JM\rangle, \quad (7)$$

where $|\mu_p J_p\rangle$ denotes the μ_p eigenvector of H_p of those having spin J_p with a similar meaning for $|\mu_n J_n\rangle$. The calculation shows that the off-diagonal matrix elements of

V_{pn} between states (7) that differ significantly in their μ_p and μ_n values are, generally, very small. Such a feature justifies the weak-coupling approximation and helps to keep the dimensions of the energy matrices relatively small. The largest matrix in our calculation occurs for the 5^- states and has dimension 972.

The matrix elements of the effective two-body interaction contained in H_p , H_n , and V_{pn} in (6) have been calculated by means of second order perturbation theory using the *Sussex* interaction³⁴ as G matrix. Details on the determination of the neutron interaction may be found in Ref. 2 while the calculation of the proton interaction is discussed in Ref. 7. Finally the matrix elements of V_{pn} have been eliminated in this work by considering the graphs shown in Fig. 7 in the space of $2\hbar\omega$ excitations.

The biggest problem in establishing the Hamiltonian in (6) is the determination of the single-particle energies contained in H_p and H_n . Normally these energies are taken directly from experiment. However in our case the one-hole nucleus $^{99}_{49}\text{In}$ and the one-particle nucleus $^{101}_{50}\text{Sn}$ are both far from the stability line and their spectra have not yet been established.

As discussed in Ref. 7 the single-hole energies can be estimated making a least-square fit to the energy spectra of the $N=50$ nuclei ^{92}Mo , ^{93}Tc , ^{94}Ru , ^{95}Rh , and ^{95}Pd . Thus treating the energies of the $1p_{1/2}$ and $1p_{3/2}$ orbitals relative to the $0g_{9/2}$ as parameters and considering 33 levels as input to the fitting procedure, one obtains⁷

$$\begin{aligned} \epsilon_{9/2} &= 0, \quad \epsilon_{1/2} = -1.26 \text{ MeV}, \\ \epsilon_{3/2} &= -2.15 \text{ MeV}. \end{aligned} \quad (8)$$

The above procedure cannot be applied to the neutron

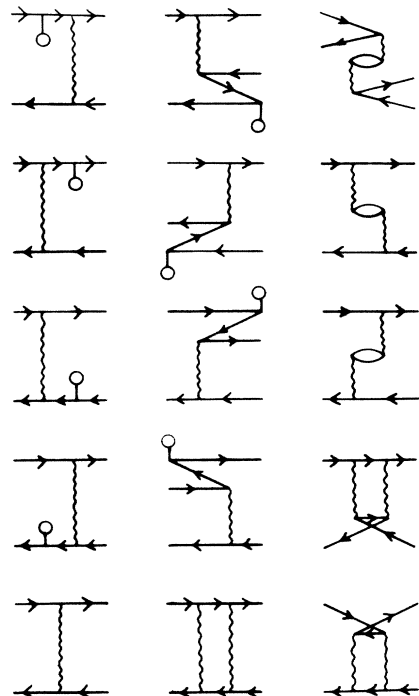


FIG. 7. Graphs involved in the determination of the effective interaction between proton holes and neutrons.

case since the nuclei with few valence neutrons outside ^{100}Sn are known very little. For this reason we have adopted the neutron energies used in previous calculations²⁻⁵ where ^{90}Zr was employed as a core and adjusted them to a ^{100}Sn core by considering the interaction of the

additional ten protons with the single neutron. Using the proton-neutron interaction of Ref. 2 we thus obtain

$$\begin{aligned} \epsilon_{5/2} &= 0, \quad \epsilon_{7/2} = 0.01 \text{ MeV}, \\ \epsilon_{1/2} &= 1.31 \text{ MeV}, \quad \epsilon_{3/2} = 1.90 \text{ MeV}. \end{aligned} \quad (9)$$

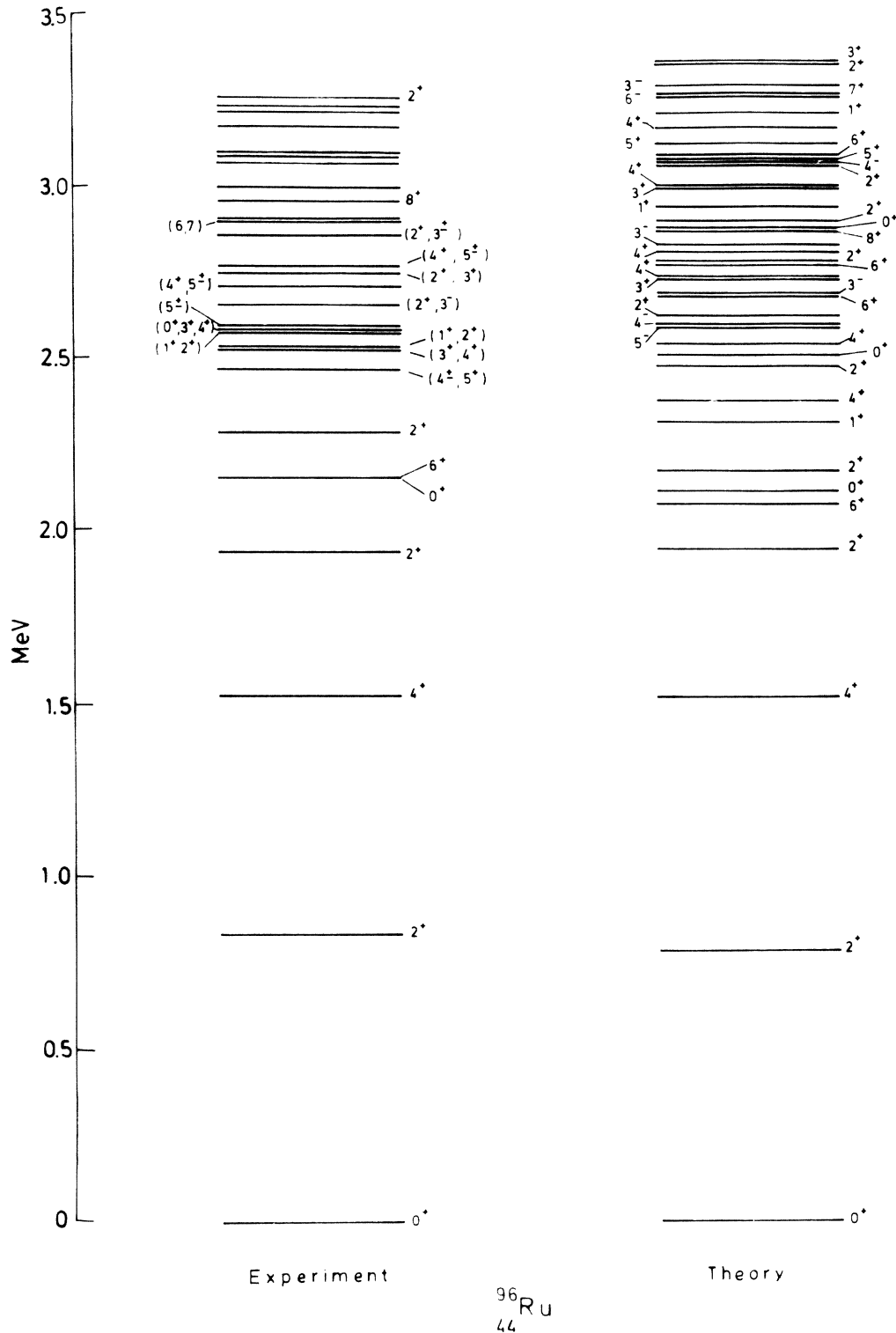


FIG. 8. The experimental and calculated spectrum of ^{96}Ru up to 3.3 MeV.

The calculated energy spectrum of ^{96}Ru is shown in Figs. 8 and 9 in comparison with experiment. Figure 8 shows all levels of ^{96}Ru that occur up to 3.3 MeV, while Fig. 9 concentrates on the high-spin ($J \geq 5$) and helps to compare the predictions of the model with the energy levels populated in heavy-ion experiments.^{9,14,15}

As both Figs. 8 and 9 show, there is, generally, a very satisfactory agreement between theory and experiment on

the level scheme of ^{96}Ru . Regarding the low-energy spectrum, the experimentally observed levels up to 2.3 MeV have all definite spin and parity assignments. As may be seen from Fig. 8 the model reproduces within 100 keV all these levels. For higher than 2.3 MeV excitation the comparison between theory and experiment becomes very difficult due to the large density of the observed levels and the many ambiguities that still exist in their J^π assign-

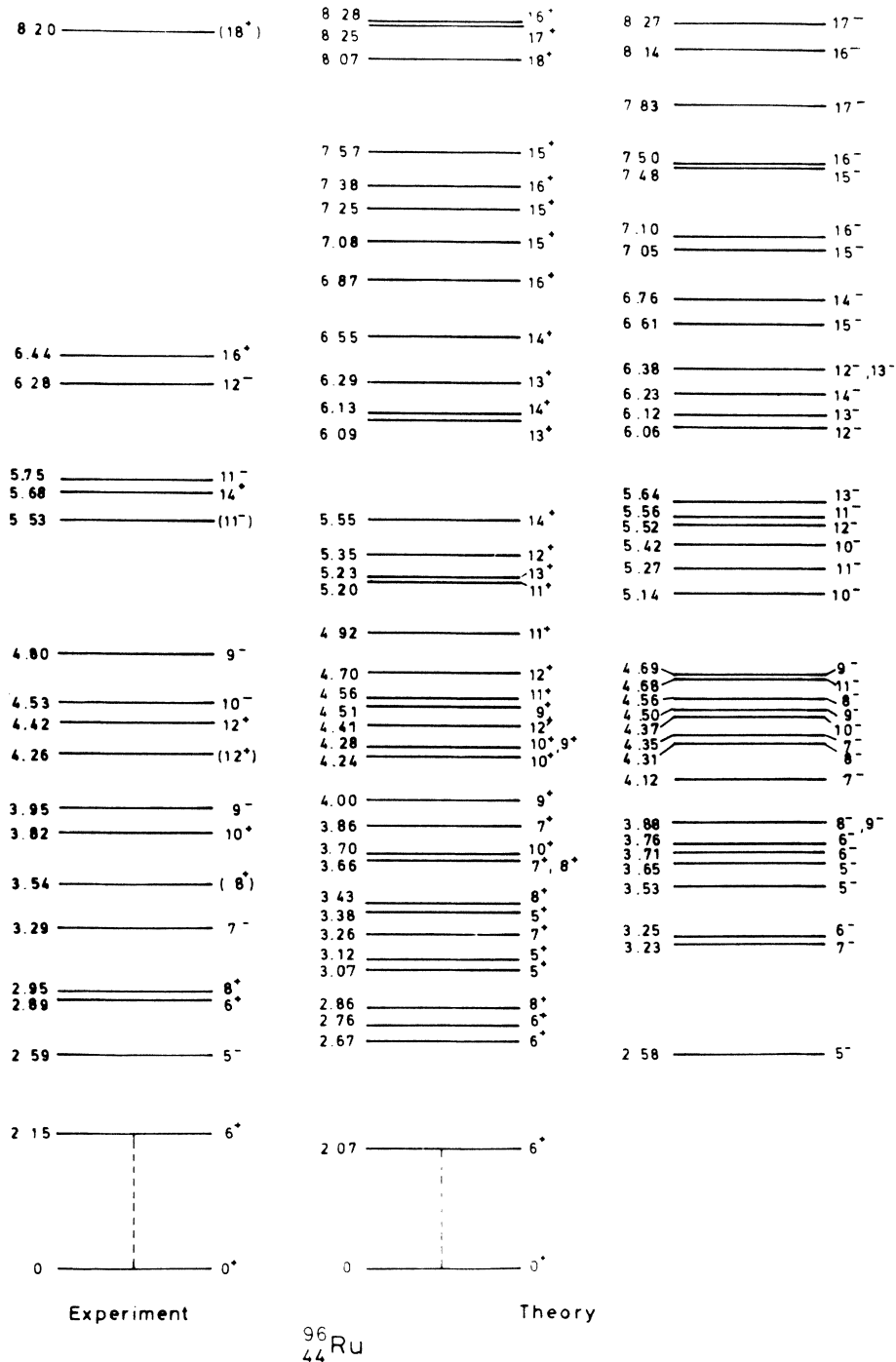


FIG. 9. The experimental and calculated spectrum for the high-spin ($J \geq 5$) states of ^{96}Ru . In the theoretical spectrum only the three lowest states for each J^π value are shown.

ments. However, as Fig. 8 shows, the model accounts for the observed density of levels while it reproduces within 200 keV most experimental levels for which some possible J^π assignment has been made. Of course, if the levels at 2528, 2576, 2650, 2739, and 2851 keV are all found to be 2^+ states, a possibility that exists as the results of Table II show, then the model fails to account for their number. The calculation predicts four 2^+ states in this energy region at about 2.47, 2.61, 2.77, and 3.05 MeV. Similarly the calculation predicts that the first 5^+ state occurs at about 3.07 MeV, while the results of Table II do not exclude the possibility that the levels observed at 2462 and 2588 keV are 5^+ states. However, as discussed below, the decay of the 2462 keV level is well accounted for by the calculation if this is a 4^+ state, an assignment which is also not excluded by the experimental results shown in

Table II. In addition the analysis of heavy ion experiments^{9,14,15} favors a 5^- assignment to the 2588 keV level. It is interesting to notice in Figs. 8 and 9 that the calculation produces a 5^- state at 2.58 MeV.

The high-spin states of ^{96}Ru that have been populated in heavy-ion experiments^{9,14,15} are primarily yrast levels. For this reason only the lowest three states of each J^π value ($J \geq 5$) have been included in the theoretical spectrum shown in Fig. 9. As this figure shows the model accounts remarkably well for the presence of all observed levels including the possible 18^+ state at 8.20 MeV. Moreover the calculation predicts a large number of additional levels including several of unnatural parity. It will be an interesting test on the validity of this model if the existence of these additional levels were to be investigated in future experiments on ^{96}Ru .

TABLE VI. List of experimental and calculated $B(M1)$ and $B(E2)$ values.

Initial state		Final state		$B(M1)$ in W.u.		$B(E2)$ in W.u.	
J^π	E (MeV)	J^π	E (MeV)	Experiment	Theory	Experiment	Theory
2^+	0.83	0^+	0.00			20.4 ± 2.0	21.7
4^+	1.52	2^+	0.83			20.9 ± 2.8	24.8
2^+	1.93	0^+	0.00				3.5×10^{-2}
		2^+	0.83	2×10^{-3}	2.6×10^{-2}	34^{+14}_{-10}	23.5
0^+	2.15	2^+	0.83			12^{+8}_{-7}	5.54
2^+	2.28	0^+	0.00				1.34
		2^+	0.83		0.55		0.52
4^+	2.46	2^+	0.83				0.29
		4^+	1.52	$0.27^{+0.11}_{-0.09}$	0.57	$1.5^{+7.0}_{-1.5}$	0.76
2^+	2.53	0^+	0.00				0.21
		2^+	0.83		1.7×10^{-2}		7.4×10^{-2}
		2^+	1.93		5.0×10^{-3}		4.0×10^{-2}
		4^+	1.52				2.6×10^{-2}
2^+	2.58	0^+	0.00				0.27
		2^+	0.83		0.11		3.0×10^{-2}
		2^+	1.93		5.0×10^{-3}		0.73
		4^+	1.52				0.19
2^+	2.65	0^+	0.00				2.6×10^{-3}
		2^+	0.83		3.9×10^{-2}		1.03
		2^+	1.93		0.22		1.73
		4^+	1.52				0.18
2^+	2.85	0^+	0.00				9.9×10^{-2}
		2^+	0.83	$(5^{+5}_{-3}) \times 10^{-3}$	8.6×10^{-3}	3.0 ± 1.6	1.1
		2^+	1.93		5.1×10^{-2}		0.17
		4^+	1.51				0.41
3^+	2.85	2^+	0.83	$(17^{+10}_{-3}) \times 10^{-3}$		$0.03^{+0.08}_{-0.03}$	
				or	2.0×10^{-2}	or	2.19
				$(26 \pm 14) \times 10^{-4}$		$3.6^{+2.0}_{-1.5}$	
		2	1.93		4.1×10^{-2}		20.5
		4	1.52		3.4×10^{-2}		4.19

It should be pointed out here that, despite the success of the calculation in reproducing the energy spectrum of ^{96}Ru , certain improvements must be introduced into the model in order to describe sufficiently all the observed properties of the ^{96}Ru levels. The way in which the calculation must be improved is best understood if one considers the electromagnetic decay of the negative parity states of ^{96}Ru . As may be seen in Tables II and V, in the energy region 2.4 to 3.0 MeV there are several possible negative parity states of ^{96}Ru and these appear to decay to positive parity states primarily via the $M2$ and $E1$ modes. However, due to the choice of the model space discussed above, the present calculation cannot account for either of these modes of decay. Thus to account for $M2$ decay one must include in the model space the $0f_{5/2}$ orbital for the

protons and/or the $0h_{11/2}$ orbital for the neutrons. The problem becomes even worse with the $E1$ mode since to account for it one must also consider the effects of various neutron orbitals like the $1f_{7/2}$, $2p_{3/2}$, \dots , plus the $0f_{7/2}$ for the protons. It is obvious that, even with drastic approximations, a calculation including these additional orbitals would be extremely difficult to attempt and for this to be justified more detailed experimental information on ^{96}Ru is certainly required.

Although, as discussed above, the present calculation cannot give a complete description of the ^{96}Ru properties, still it is interesting to compare with experiment its predictions on the decay of the low lying positive parity states of this nucleus. This is because one expects that the additional configurations, described above, will appear

TABLE VII. Experimental and calculated electromagnetic properties of ^{96}Ru levels.

Initial State		Final state		$\delta(M1/E2)^a$		Branch (%)		T (psec)	
J	E (MeV)	J	E (MeV)	Expt.	Theor.	Expt.	Theor.	Expt.	Theor.
2 ⁺	0.83	0 ⁺	0.00			100	100		3.5
4 ⁺	1.52	2 ⁺	0.83			100	100	10.0±1.3	8.1
2 ⁺	1.93	0 ⁺	0.00			0	1.3		
		2 ⁺	0.83	-5.2 ^{+1.0} _{-1.4}	1.07	100	98.7	0.55 ^{+0.22} _{-0.16}	0.43
0 ⁺	2.15	2 ⁺	0.83			100	100	0.66 ^{+0.81} _{-0.26}	1.4
2 ⁺	2.28	0 ⁺	0.00			7	4.8		
		2 ⁺	0.83	0.03±0.10	-0.05	93	95.2		0.02
4 ⁺	2.46	2 ⁺	0.83			0	0.7		
		4 ⁺	1.52	-0.07 ^{+0.12} _{-0.10}	-0.03	100	99.3	0.14 ^{+0.07} _{-0.04}	0.07
2 ⁺	2.53	0 ⁺	0.00			23	20.7		
		2 ⁺	0.83	-0.34±0.09	-0.12	77	78.3		
		4 ⁺	1.52			0	0		
		2 ⁺	1.93		0.05	0	1.0		0.30
2 ⁺	2.58	0 ⁺	0.00			30	5.2		
		2 ⁺	0.83	0.04±0.12	0.03	70	94.6		
		4 ⁺	1.52			0	0		
		2 ⁺	1.93	2.0 ^{+0.6} _{-0.5}	0.25	0	0.2		0.05
2 ⁺	2.65	0 ⁺	0.00			0	0.1		
		2 ⁺	0.83	-0.60	-0.30	74	75.6		
		4 ⁺	1.52			12	0.1		
		2 ⁺	1.93		0.06	14	24.2		0.09
2 ⁺	2.85	0 ⁺	0.00			0	11.3		
		2 ⁺	0.83	-1.6 ^{+0.6} _{-0.4}	-0.73	90	64.2		
		4 ⁺	1.52			0	1.0		
		2 ⁺	1.93		0.05	10	23.5	0.20 ^{+0.14} _{-0.07}	0.19
3 ⁺	2.85	2 ⁺	0.83	-0.08 ^{+0.06} _{-0.07}	-0.68	90	62.6		
				or					
				-2.4 ^{+0.4} _{-0.5}					
		4 ⁺	1.52		0.47	0	25.5		
		2 ⁺	1.93		0.66	10	11.9	0.20 ^{+0.14} _{-0.07}	0.08

^aThe experimental values of δ that are not found in Table V are taken from Lange *et al.* (Ref. 17).

only as very small admixtures in the wave functions of these states. Moreover such a comparison is practicable since, as Tables IV and V show, the electromagnetic properties of the low-lying states of ^{96}Ru are better known experimentally.

The theoretical predictions on the electromagnetic decay of the low-lying positive parity levels of ^{96}Ru are compared with experiment in Tables VI and VII. Table VI lists experimental and calculated $B(M1)$ and $B(E2)$ values, while Table VII lists values of $\delta(E2/M1)$ ratios, branching ratios and lifetimes. As may be checked in Tables II and V and also in Ref. 17, there are enough data in the decay of the 2462, 2528, 2576, 2650, and 2851 keV levels that, despite the fact that these levels have not yet been assigned a definite J^π value, one may attempt to identify them with theoretical states. In the results shown in Tables VI and VII the 2462 keV level is identified with the second theoretical 4^+ state predicted to be at about 2.37 MeV, while the 2528, 2576, and 2650 keV levels are identified with the 2_4^+ , 2_5^+ , and 2_6^+ that appear at 2.47, 2.61, and 2.77 MeV in the theoretical spectrum, respectively. Finally the 2851 keV level is considered to be either a 2^+ or a 3^+ state and thus is identified with the 2_7^+ and the 3_2^+ theoretical states predicted to be at about 3.07 and 2.89 MeV, respectively.

In the calculation of $M1$ rates the bare $M1$ operator has been used. On the other hand, agreement with experiment on $E2$ rates can be obtained only through the introduction of effective charges. For simplicity a common effective charge has been assigned to both protons and neutrons and this quantity has been treated as an adjustable parameter. It was found in this way that a charge of 1 added to the natural charge of the particles produces best overall agreement with experiment.

As may be seen in Table VI, the predictions of the calculation on $B(E2)$ values are in very satisfactory agreement with experiment in all cases where an experimental estimate is available. Also the calculation produces a value of -0.24 e b for the quadrupole moment of the 2_1^+ state which is in fair agreement with the experimental value of -0.13 ± 0.09 e b.²⁰ The same agreement is not observed, however, in the case of $M1$ decay where, as Table VI shows, all theoretical $B(M1)$ values are predicted to be larger than the experimental ones. The worse disagreement appears in the decay of the second 2^+ state at 1.93 MeV where the theoretical $B(M1)$ value is an or-

der of magnitude larger from the experimental estimate. However it should be noticed in this case that the experimental $B(M1)$ is a very small quantity. Such a feature suggests that small changes in the wave functions of the 2_1^+ and 2_2^+ states could shift the theoretical $B(M1)$ towards the experimental value. An interesting feature appears also in the decay of the 2.85 MeV level, if this is assumed to be a 3^+ state. In this case, as Table VI shows, the calculation produces $B(M1)$ and $B(E2)$ values that are both close to the larger of the two experimental estimates but which, however, are not compatible among themselves.

A final comparison between theory and experiment on the decay of the ^{96}Ru levels is made in Table VII. As the results of this table show, the calculation accounts satisfactorily for most of the electromagnetic properties of the established levels of ^{96}Ru up to 2.28 MeV. The only exception in this agreement occurs for the $\delta(E2/M1)$ ratio in the decay of 1.93 MeV state for which the calculation not only underestimates its magnitude but also produces the wrong sign. As discussed above, this failure is due to the inability of the present calculation to reproduce the observed $M1$ mode in the $2_2^+ \rightarrow 2_1^+$ decay.

As may be seen from Table VII, the decay of the 2.46 and 2.53 MeV levels is well understood in terms of the present calculation provided these states are confirmed to have a 4^+ and a 2^+ assignment, respectively. On the other hand the 2^+ assignment to the 2.58 and 2.65 MeV levels is not well understood in terms of the theoretical results, shown in Table VII, which fail to account for the 30% branch observed in the decay of the 2.58 MeV level to the ground state and the 12% branch in the decay of the 2.65 MeV level to the 4^+ at 1.52 MeV. Finally the results shown in Table VII with respect to the 2.85 MeV level, clearly suggest that the model is unable to reproduce the observed branching ratios in the decay of this state if the latter is found to be a 2^+ or a 3^+ state.

ACKNOWLEDGMENTS

Thanks are due to Dr. T. Anagnostopoulos for valuable help with the computer programs. The authors also gratefully acknowledge financial support from the International Atomic Energy Agency.

¹A. C. Xenoulis and D. G. Sarantites, *Phys. Rev. C* **7**, 1193 (1973); D. G. Sarantites and A. C. Xenoulis, *ibid.* **10**, 2348 (1974).
²L. D. Skouras and C. Dedes, *Phys. Rev. C* **15**, 1873 (1977); C. Dedes and L. D. Skouras, *Phys. Lett.* **66B**, 417 (1977).
³A. C. Xenoulis and C. A. Kalfas, *Phys. Rev. C* **20**, 145 (1979).
⁴C. A. Kalfas, A. C. Xenoulis, E. Adamides, S. Papaioannou, and L. D. Skouras, *Z. Phys. A* **292**, 153 (1979).
⁵E. Adamides, L. D. Skouras, and A. C. Xenoulis, *Phys. Rev. C* **23**, 2016 (1981); **24**, 1429 (1981).
⁶E. Adamides, W. McLatchie, R. Skensved, and J. R. Leslie, *Phys. Rev. C* **30**, 1153 (1984).
⁷J. Sinatkas, L. D. Skouras, D. Strottman, and J. D. Vergados

(unpublished).

⁸T. A. Doron and M. Blann, *Nucl. Phys.* **A167**, 577 (1971).
⁹T. A. Walkiewicz, S. Raman, and J. B. McGrory, *Phys. Rev. C* **27**, 1710 (1983).
¹⁰A. H. W. Aten, Jr. and J. C. Kapteyn, *Physica (Utrecht)* **33**, 705 (1967).
¹¹S. C. Gujrathi, C. Weiffenbach, and J. K. P. Lee, *J. Phys. G* **1**, 67 (1975).
¹²J. Ashkenazi, E. Friedman, D. Nir, and J. Zioni, *Nucl. Phys.* **A186**, 321 (1970).
¹³L. R. Medsker, *Nucl. Data Sheets* **8**, 599 (1972).
¹⁴C. M. Lederer, J. M. Jaklevic, and J. M. Hollander, *Nucl. Phys.* **A169**, 449 (1971).

- ¹⁵W. F. Piel, Jr. and G. Scharff-Goldhaber, *Phys. Rev. C* **30**, 902 (1984).
- ¹⁶A. H. Lumpkin, L. H. Harwood, L. A. Parks, and J. D. Fox, *Phys. Rev. C* **17**, 376 (1978).
- ¹⁷J. Lange, J. Neuber, P. Tendler, C. D. Uhlhorn, A. T. Kandil, and H. V. Buttlar, *Nucl. Phys. A* **330**, 29 (1979).
- ¹⁸S. Landsberger, R. Lecompte, P. Paradis, and S. Monaro, *Phys. Rev. C* **21**, 588 (1980).
- ¹⁹F. K. McGowan, R. L. Robinson, P. H. Stelson, and W. T. Millner, *Nucl. Phys. A* **113**, 259 (1968).
- ²⁰C. Fahlander, L. Hasselgren, G. Possnert, and J. E. Thun, *Phys. Scr.* **18**, 47 (1978).
- ²¹W. Hauser and H. Feshbach, *Phys. Rev.* **87**, 366 (1952).
- ²²J. B. Ball and K. H. Bhatt, private communication cited in Ref. 8.
- ²³E. Sheldon and R. M. Strang, *Comput. Phys. Commun.* **1**, 35 (1969).
- ²⁴A. S. Mani, M. A. Melkanoff, and I. Iori, *Commisariat a l'Energie Atomique Report No. 2379*, 1963 (unpublished).
- ²⁵F. James and M. Roos, CERN Report NO. B506, 1971 (unpublished).
- ²⁶D. W. Rogers, *Nucl. Instrum. Methods* **127**, 253 (1975).
- ²⁷K. S. Krane and R. M. Steffen, *Phys. Rev. C* **2**, 724 (1970).
- ²⁸C. Moazed, T. Becker, P. A. Assimakopoulos, and D. M. Van Patter, *Nucl. Phys. A* **169**, 651 (1971).
- ²⁹A. E. Blauground, *Nucl. Phys.* **88**, 501 (1966).
- ³⁰L. Lindhard, M. Sharff, and H. E. Schiott, *K. Dan. Vidensk. Selsk., Mat-Fys. Medd.* **33**, No. 14 (1963).
- ³¹D. G. Sarantites, J. H. Barker, N.-H. Lu, E. J. Hoffman, and D. M. Van Patter, *Phys. Rev. C* **8**, 629 (1973).
- ³²A. Bohr, *K. Dan. Vidensk. Selsk., Mat-Fys. Medd.* **26**, No. 14 (1952).
- ³³A. Bohr and B. R. Mottelson, *K. Dan. Vidensk. Selsk., Mat-Fys. Medd.* **27**, No. 16 (1953).
- ³⁴J. P. Elliott, A. D. Jackson, H. A. Mavromatis, E. A. Sander-son, and B. Singh, *Nucl. Phys. A* **121**, 241 (1968).